Jurnal Teknologi, 41(F) Keluaran Khas. Dis. 2004: 49–60

CHARACTERISTIC OF CO-POLYAMIDE NANOFILTRATION MEMBRANE: THE EFFECT OF REACTION TIME

A. L. AHMAD[1*], B. S. OOI[2], M. M. D. ZULKALI[3] & J. P. CHOUDHURY[4]

Abstract. Modified polypiperazinamide nanofiltration membranes were fabricated under different reaction time. The membranes were characterized for its pore size and effective thickness/porosity using Donnan Steric Pore Flow Model. The pore size was reduced initially due to the crosslinking process but becomes larger at longer reaction time because of the weaker pores wall. On the other hand, the effective thickness/porosity grows with polymerization time and becomes constant after 60s. The effect of reaction time on the pore size is not as significant as effective thickness/porosity. Within 2 minutes of polymerization time, the effective thickness of the barrier layer would vary about 150%.

Keywords: Nanofiltration, reaction time, pore size, effective thickness/porosity

Abstrak. Membran penurasan nano yang diubahsuai daripada polipiperazinamida telah dihasilkan dalam masa tindakbalas yang berbeza. Membran berkenaan dicirikan terhadap liang saiz dan ketebalan berkesan/keporosan dengan menggunakan model DSPM. Liang membran menjadi kecil pada permulaan tindakbalas disebabkan proses pengaitan bersilang tetapi liang saiz akan bertambah untuk jangkamasa tindakbalas yang lebih lama kerana kelemahan dinding liang membran. Walau bagaimanapun, nilai ketebalan berkesan/keporosan bertambah dengan masa dan menjadi stabil selepas 60s. Kesan masa tindakbalas terhadap liang saiz adalah tidak ketara berbanding dengan kesannya terhadap ketebalan berkesan/keporosan. Selama 2 minit tindakbalas, nilai ketebalan berkesan/keporosan untuk lapisan penapis berubah sebanyak 150%.

Kata kunci: Penurasan Nano, masa tindakbalas, saiz liang, ketebalan berkesan/keporosan

1.0 INTRODUCTION

Nanofiltration (NF) can be considered as a relatively new type of pressure driven membrane compared to reverse osmosis and ultrafiltration. Higher flux and lower operating pressure of nanofiltration make the membrane become, feasible to be applied in both water and wastewater treatment process. Nowadays, nanofiltration has been used widely in drinking water industry [1] and wastewater treatment for removal of contaminants such as pesticides [2], arsenic [3], soil leachate [4], and dyes [5]. Recently,

[1,2,3 & 4]School of Chemical Engineering, Engineering Campus, Universiti Sains Malaysia, Seri Ampangan, 14300 Nibong Tebal, S.P.S, Penang, Malaysia.
[1*] Corresponding author: E-mail: chlatif@eng.usm.my

nanofiltration membranes are also studied for applications in food [6] and bio-process [7] purposes.

By definition, the pore size of NF membranes is around 1 nm. Since the pores are so small, the electrostatic interactions between the membrane material and ions in solution are likely to play a significant role on the electrolyte transport through the membrane pores [8]. Therefore, for ionic solutes, the interactions between the solutes and the membrane cannot be governed by steric hindrance alone. Electrolyte transport mechanisms through nanofiltration membranes should be investigated in terms of convection, diffusion, and electromigration.

According to the Donnan Steric Pore Flow Model, the membranes are assumed to consist of a bundle of identical straight cylindrical pores. The neutral solute transports through the membrane effective layer are controlled by the pore size (r_p) and effective thickness/porosity ($\Delta x/A_k$). By understanding membrane fabrication conditions like reactant concentration and reaction time, membrane with specific characteristic (r_p and $\Delta x/A_k$) could be tailor-made.

Interfacial polymerization (IP) technique is one of the techniques used in preparing composite nanofiltration membranes. The membranes produced are high in water permeation flux and salt rejection. There are several advantages in making membrane using the IP process. The IP film, which forms the selectively permeable barrier layer can be made quite thin, to less than 0.1 μm [9]. The thin film composite (TFC) membranes made by the IP process also offers good selectivity and high permeability of water. Besides, IP technique allows the properties of the permselective barrier layer to be optimized independently from the supporting layer.

It was found that the critical parameters for thin film coating are the reaction time, relative humidity, and the coating temperature. These parameters play an important role in determining the structure of the interfacially polymerized surface film and subsequently, the membrane's performance [10, 11]. Up to now, several studies have tried to relate the membrane performance to the reaction time. However a few studies have been carried out to look into the effect of reaction time on pore size and effective thickness/porosity. This relationship is very important in order to explore the behaviour of flux and rejection in nanofiltration membrane. The objective of this paper, therefore, is to study the effect of reaction time on the membranes characteristics like the pore size and effective thickness/porosity using Donnan Steric Pore Flow Model.

2.0 THEORY

2.1 Model Assumptions

In order to determine the pore size and effective thickness/porosity, Donnan Steric Pore Flow Model (DSPM) was used [12, 13]. Below are the assumptions applied to the derivation of DSPM model:

- The membrane consists of a bundle of identical straight cylindrical pores of radius r_p and length Δx.
- A very diluted system was used, which enable the coupling effect between the components in the solution to be neglected
- For porous membranes, the fluxes, concentrations, potentials, and velocity were all defined in terms of radially averaged quantities.

2.1 Fundamental Equations of DSPM

The solute velocity was assumed to be fully developed inside the pore and had the parabolic profile of the Hagen-Poiseuille type. K_{id} and K_{ic} are related to the hydrodynamic coefficients as:

$$K_{id} = K^{-1}(\lambda,0) = 1.0 - 2.30\lambda + 1.154\lambda^2 + 0.224\lambda^3 \quad (1)$$

$$K_{ic} = (2-\Phi)G(\lambda,0) = 1.0 + 0.054\lambda - 0.988\lambda^2 + 0.441\lambda^3 \quad (2)$$

For neutral solute (glucose), the solute flux through the membrane could be expressed as:

$$j_i = -D_{ip}\frac{dc_i}{dx} + K_{ic}c_i J_v \quad (3)$$

For purely steric interactions between the solute and the pore wall, Φ is the steric terms relating to the finite size of the solute and the pore size.

$$\Phi = (1-\lambda)^2 \quad (4)$$

where λ is a ratio of solute radius, r_s (m) to pore size, r_p (m). In terms of real rejection, Equation(3) becomes,

$$R_{real} = 1 - \frac{C_{i,p}}{C_{i,m}} = 1 - \frac{K_{i,c}\Phi}{1-\exp(-Pe_m)\left[1-\Phi K_{i,c}\right]} \quad (5)$$

where $C_{i,m}$ and $C_{i,p}$ are concentration on the feed side of membrane (mol m^{-3}) and concentration in permeate (mol m^{-3}) respectively. The peclet number, Pe_m is defined as:

$$Pe_m = \frac{K_{i,c}}{K_{i,d}}\frac{J_v \Delta x}{D_{i,\infty}A_k} \quad (6)$$

where $D_{i\infty}$ is the bulk diffusivity ($m^2 s^{-1}$), J_v is the volume flux (based on membrane area)($m.s^{-1}$), Δx is the effective thickness, (m) and A_k is porosity of the membrane.

The Hagen-Poiseuille equation gives the relationship between the pure water flux and the applied pressure across the membrane[14].

$$J_w = \frac{r_p^2 \Delta P}{8\mu(\Delta x / A_k)} \tag{7}$$

where J_w is the water flux (m.s^{-1}), ΔP is the applied transmembrane pressure (kPa), and μ is the viscosity of the solution (kPa.s).

To find the film layer concentration, the concentration polarization equation was employed. For a stirred cell configuration, the observed rejection was related to the real rejection by volume flux, J_v, and the mass transfer coefficient, k, as follows [12];

$$\ln\left(\frac{1-R_{obs}}{R_{obs}}\right) = \ln\left(\frac{1-R_{real}}{R_{real}}\right) + \frac{J_v}{k} \tag{7}$$

$$k = k'\omega^{0.567} \tag{8}$$

where,

$$k' = 0.23\left(\frac{r^2}{v}\right)^{0.567}\left(\frac{v}{D_\infty}\right)^{0.33}\frac{D_\infty}{r} \tag{9}$$

where k', ω, r, and v are mass transfer coefficient (m s^{-1}), stirring speed (s^{-1}), stirrer radius (m), and kinematic viscosity (m^{2}s^{-1}) respectively.

3.0 MATERIALS AND METHODS

3.1 Material

The polysulfone Udel P-1700 (Mn : 17,000) is a product of Union Carbide Corporation. Piperazine, 3,5-diaminobenzoic acid, n-hexane, sodium chloride, and glucose were supplied by Merck Company. N-methylpyrrolidone and trimesoyl chloride were purchased from Fluka and polyvinylpyrrolidone, from Sigma-aldrich Co. The tightly woven polyester, style 0715 Dacron Fabric was supplied by Texlon Corporation (USA).

3.2 Preparation of Polysulfone Support Layer

The polysulfone support was prepared by dissolving 15% polysulfone (Udel P-1700) in N-methylpyrrolidone with 18% polyvinylpyrrolidone as a pore-former agent. The solution was casted onto a tightly woven polyester fabric with a thickness of 150 μm. Then, the membrane was immersed into a water bath and kept there for 24 hours until most of the solvent and water soluble polymer were removed[15].

3.3 Fabrication of Thin Film Composite Membranes

The support layer which was taped on a glass plate was immediately dipped into an aqueous diamine solution containing 2w/w% piperazine(PIP) and 0.1w/w% 3,5-diaminobenzoic acid (BA) for 5 minutes at ambient temperature. The excess solution from the impregnated membrane surface was removed using a rubber roller. The membrane was then dipped into the n-hexane solution, which consists of 0.1w/v% trimesoyl chloride(TMC). The reaction was carried out at predetermined time of 5, 10, 15, 30, 45, 60, 75, and 120s.

3.4 Membrane Permeation Characterization

Membrane permeation test was carried out using the Amicon 8200 stirred cell at five different pressures: 150kPa, 250kPa, 350kPa, 400kPa, and 450kPa. The membrane was cut to a diameter of 5.5 cm (effective area of 28.27cm^2), and then, mounted at the bottom of the stirred cell. For each operating pressure, deionised water and fresh glucose solution were used as the feed solution. Bulk feed concentration was calculated based on the average of initial and final feed concentration. Nitrogen gas was used to pressurize the water flux through the membrane. The solution was stirred at the speed of 350 rpm to reduce concentration polarization. The feed solutions are pure water, 0.001M NaCl, 0.01M NaCl, 0.1M NaCl solution, and 300 ppm glucose solution. The NaCl permeate concentrations were measured using the conductivity meter (Hanna Instruments, Italy, Model: HI8633) while glucose permeate concentration was analyzed using the spectrophotometer (Thermo Spectronic, USA, Model: GENESYS 20) at 485 nm.

Each membrane was subjected for pressure pre-treatment at 500kPa for 1 hour before the permeation experiments. The flux was equilibrated for the passage of first 20 ml permeates and the following 10 ml permeate was collected for concentration analysis.

3.5 Determination of r_p and $\Delta x/A_k$ using Uncharged Solute (Glucose)

In this approach, an average pore size (r_p) was fitted by solving Equation (7)-(9) with pure water flux, J_w versus ΔP giving the slope of:

$$slope = \frac{r_p^2}{8\mu\left(\Delta x / A_k\right)} \tag{10}$$

and

$$\Delta x / A_k = \frac{r_p^2}{8\mu \times slope} \tag{11}$$

Substitute Equation (11) into Equation (6) and get the r_p value by best fitting the J_v-R_{real} curve of glucose solution based on Equation (5). The radius of solute (glucose) was obtained from the literature [12] as 0.365 nm. The $\Delta x/A_k$ value could be obtained directly from the permeability data Equation (7).

4.0 RESULTS AND DISCUSSION

The effect of polymerization time on rp and $\Delta x/A_k$ are shown in Figures 1 and 2, respectively. Figure 1 shows that below 60s of reaction time, the effect of polymerization time on pore size was not significant. However, there is a slightly drop in the pore size from 5 to 15s. The pore size tends to grow at the reaction time beyond 75s.

Initially, as reaction time increases (<15s), the polymer layer tends to be cross-linked to produce a tighter membrane with smaller pore size. At longer reaction time (>75s), an adverse trend was observed. This phenomenon can be explained by looking at the slower reactivity of 3,5-diaminobenzoic acid compared to piperazine. The electron-drawing carboxylic group in BA made the diamine functional group less neucleophilic, therefore, reducing its reactivity. At longer reaction time, the content of BA in the polyamide skin layer increased. Higher content of BA leads to a higher ratio of hydrophilic group in the membrane [16]. Consequently, exceeding water uptake produced the pores with weaker pore wall. The adjacent pores wall would coalescent together to produce an average bigger pore size. This explained why at higher polymerization time, poorer rejection was obtained.

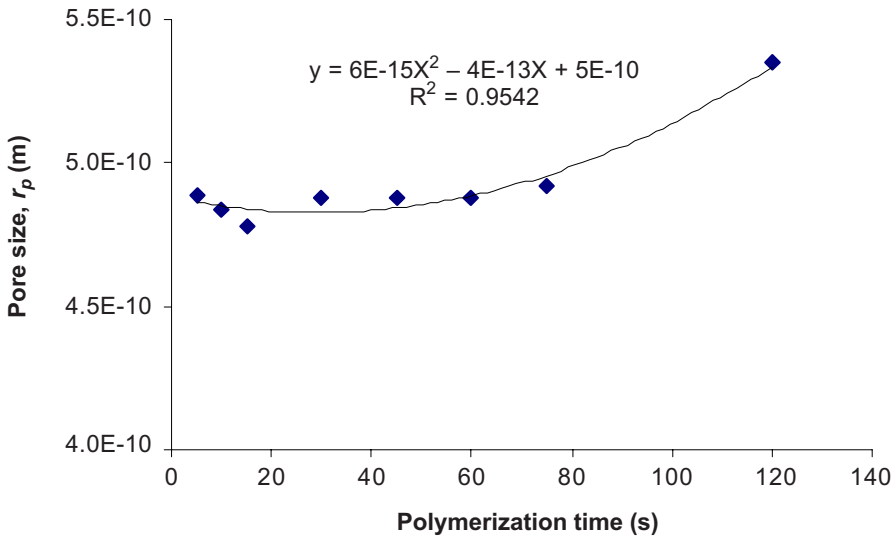

Figure 1 Effect of polymerization time on the membrane pore size

In overall, polymerization time is not an important parameter in determining the pore size. The pore size in the study range (5 to 120s) differs about 12 % only with an average of 0.5 nm. The pore size of the membranes produced are in the same category as the market available nanofiltration like Desal-5, NF-40, and UTC-20[17,18]. Therefore, the membranes could be classified as the tight nanofiltration membrane.

On the other hand, the effect of polymerization time on the membrane thickness was more significant. If the porosity of the membrane was assumed to be united, then, within this polymerization time, the effective thickness of the barrier layer would vary about 150 %, as shown in Figure 2.

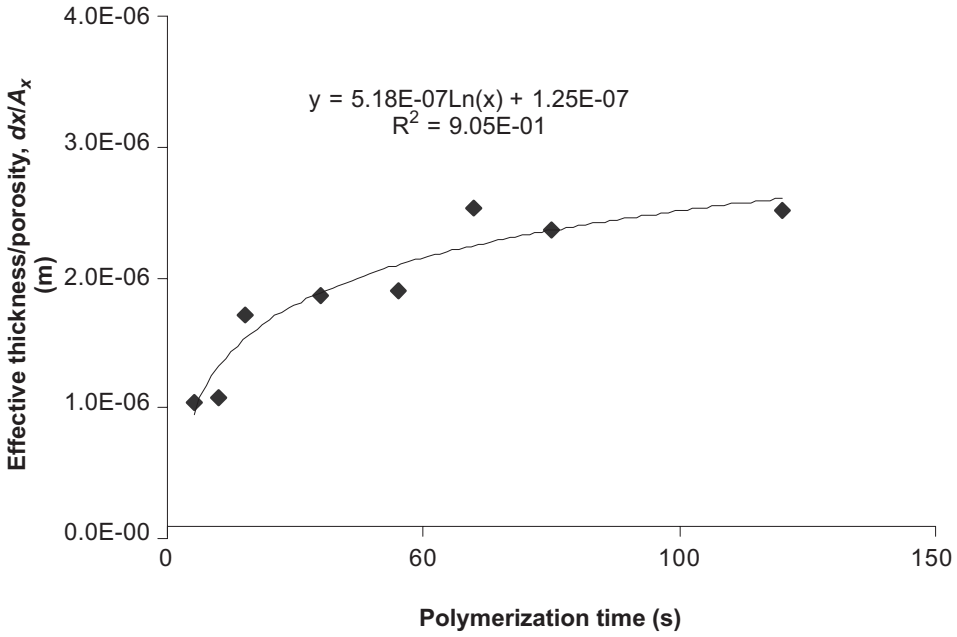

Figure 2 Effect of polymerization time on the membrane effective thickness/porosity

From Figure 2, it was noted that the effective layer grows with polymerization time. The rate of layer formation was high below 15s and started to level-off beyond 75s polymerization time. This might be due to the reaction becoming diffusion control at thicker skin layer and film growth becoming self-limiting owing to the inability of the two reactants to interpenetrate, after sufficient densification has occurred toward the organic side of the membrane [18]. It was also postulated that the reducing $\Delta x/A_k$ was caused by the increasing porosity.

As shown in Figure 1, the pore size turned out to be bigger after 60s of reaction time which contributed to a more porous membrane. It was further proved from Figure 3 that there was a significant increase in the skin layer thickness from 5 to 60s.

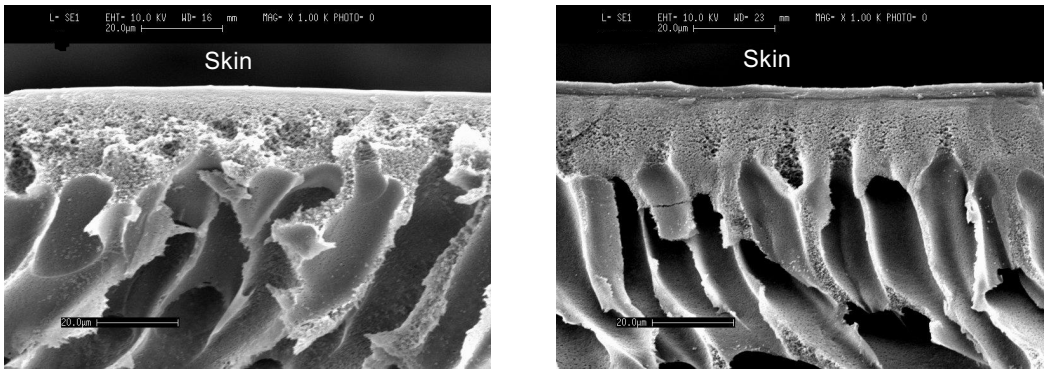

(a) (b)

Figure 3 Morphology of the membrane prepared under (a) 5s and (b) 60s

The growth of the film could be expressed in the below terms (assume unity porosity):

$$\Delta x = 5.18\times10^{-7}\ln(t)+1.25\times10^{-7} \quad (10)$$

where Δx is the effective membrane thickness (m) and t is the polymerization time (s). The resulted pores size and effective thickness/porosity under different polymerization time is tabulated as below (Table 1):

Table 1 Tabulated result of the pore size and effective thickness/porosity for membrane at different reaction time

Polymerization time, s	Pore size (´ 10^{-9}m)	Effective thickness/ porosity (´ 10^{-6}m)
5	4.89	1.036
10	4.84	1.072
15	4.78	1.715
30	4.88	1.856
45	4.88	1.894
60	4.88	2.533
75	4.92	2.372
120	5.35	2.510

The interfacial polymerised (IP) film which forms the selectively permeable layer can be made quite thin (0.1< μm)[19]. However, in this system, to produce a skin layer of about 0.1 μm, the reaction time calculated from Equation (10) would be 0.95s. A parameter that seems difficult to be controlled solely by reaction time because of the

high film growth rate. Therefore, other parameters like reactant concentration should be investigated.

5.0 CONCLUSION

The effect of polymerization time on the pore size is not as significant as compared to its effect on effective thickness/porosity. The pore size was reduced initially because of the crosslinking process between the reactants but at longer polymerization time, the pores tend to coalescent to produce a bigger pore size. On the other hand, the effective thickness/porosity grew exponentially with polymerization time. The effect is crucial with approximately 150 % of increament in $\Delta x/A_k$ within 2 minutes of reaction time. The growth of the film could be expressed in the exponential terms as $\Delta x = 5.18 \times 10^{-7} \ln (t) + 1.25 \times 10^{-7}$ if unity porosity was assumed.

NOTATION

A_k	porosity of the membrane
c_i	concentration in the membrane (mol m^{-3})
$C_{i,m}$	concentration on the feed side of membrane (mol m^{-3})
$C_{i,p}$	concentration in permeate (mol m^{-3})
$D_{i,p}$	hindered diffusivity (m^2s^{-1})
$D_{i\infty}$	bulk diffusity (m^2s^{-1})
j_i	solute flux (based on the membrane area) (mol $m^{-2}s^{-1}$)
J_v	volume flux (based on the membrane area) ($m^3m^{-2}s^{-1}$)
J_w	water flux (based on the membrane area) ($m^3m^{-2}s^{-1}$)
k	mass transfer constant (ms^{-1})
k'	mass transfer constant defined by Equation (9)
K^{-1}	the hydrodynamic enhanced drag coefficient
K_{ic}	hindrance factor for convection
K_{id}	hindrance factor for diffusion
Pe_m	peclet number
r	radius of stirrer
r_p	effective pore radius (m)
r_s	stokes radius of solutes or ions (m)
R_{obs}	observed rejection
R_{real}	real rejection
x	distance normal to membrane (m)

Δx effective membrane thickness (m)

Φ steric partition term

λ ratio of solute radius/pore radius

ω stirring speed

ACKNOWLEDGEMENTS

The authors are grateful to the financial support provided by the Ministry of Science and Technology Malaysia through its Fundamental Research and IRPA grants.

REFERENCES

[1] Paugam, L., S. Taha, J. Cabon, and G. Dorange. 2002. Elimination of Nitrate Ions in Drinking Waters by Nanofiltration. *Desalination.* 152: 271-274.

[2] Bruggen, B. V. D., K. Everaert, D. Wilms, and C. Vandecasteele. 2001. Application of Nanofiltration of Removal of Pesticides, Nitrate and Hardness from Ground Water : Rejection Properties and Economic Evaluation. *Journal of Membrane Science.* 193: 239-248.

[3] Vrijenhoek, E. M., and J. J. Waypa. 2000. Arsenic Removal from Drinking Water by a "Loose" Nanofiltration membrane. *Desalination.* 130: 265-277.

[4] Volchek, K., D. Velicogna, A. Obenauf, A. Somers, B. Wong, and A. Y. Tremblay. 2002. Novel Applications of Membrane Processes in Soil Cleanup Operations. *Desalination.* 147: 123-126.

[5] Akbari, A., J. C. Remigy, and P. Aptel. 2002. Treatment of Textile Dye Effluent using a Polyamide-based Manofiltration Membrane. *Chemical Engineering and Processing.* 41: 601-609.

[6] Nguyen, M., N. Reynolds, and S. Vigneswaran. 2003. By-product Recovery from Cottage Production by Nanofiltration. *Journal of Cleaner Production.* 11: 803-807.

[7] Zhang, W., G. He, P. Gao, and G. Chen. 2003. Development and Characterization of Composite Nanofiltration Membranes and Their Application in Concentration of Antibiotics. *Separation and Purification Technology.* 30: 27-35.

[8] Szymczyk, A., C. Labbez, P. Fievet, A. Vidonne, A. Foissy, and J. Pagetti. 2003. Contribution of Convection, Diffusion and Migration to Electrolyte Transport through Nanofiltration Membranes. *Advanced Colloid and Interface Science.* 103: 77-94.

[9] Tomaschke, J. E. 1989. Interfacially Synthesized Reverse Osmosis Membrane Containing an Amine Salt and Processes for Preparing the Same. *US Patent* 4,872,984.

[10] Jayarani, M. M., and S. S. Kulkarni. 2000. Thin-film Composite Poly(esteramide)-based Membranes. *Desalination.* 130: 17-30.

[11] Rao, A. P., S. V. Joshi, J. J. Trivedi, C. V. Devmurari, and V. J. Shah. 2003. Structure-performance Correlation of Polyamide Thin Film Composite Membranes : Effect of Coating Conditions on Film Formation. *Journal of Membrane Science.* 211: 13-24.

[12] Bowen, W. R., A. W. Mohammad and N. Hilal. 1997. Characterization of Nanofiltration Membranes for Predictive Purposes-use of Salts, Uncharged Solutes and Atomic Force Microscopy. *Journal of Membrane Science.* 126: 91-105.

[13] Mohammad, A. W., N. Ali and N. Hilal. 2003. Investigating Characteristics of Increasing Molecular Weight Cutoff Polyamide Nanofiltration Membranes using Solutes Rejection and Atomic Force Microscopy. *Separation Science and Technology.* 38: 1307-1327.

[14] Nakao S., and S. Kimura. 1981. Analysis of Solutes Rejection in Ultrafiltration. *Journal of Chemical Engineering Japan.* 14: 32-37.

[15] Kim, C. K., J. H. Kim, I. J. Roh, and J. J. Kim. 2000. The Changes of Membrane Performance with Polyamide Molecular Structure in the Reverse Osmosis Process. *Journal of Membrane Science.* 165: 189-199.

[16] Ahmad, A. L., B. S. Ooi, and J. P. Choudhury. 2003. Preparation and Characterization of Co-polyamide Thin Film Composite Membrane from Piperazine and 3,5-diaminobenzoic Acid. *Desalination.* 158: 101-108.

[17] Wang, X. L., T. Tsuru, M. Togoh, S. I. Nakao, and S. Kimura. 1995. Evaluation of Pore Structure and Electrical Properties of Nanofiltration Membranes. *Journal of Chemical Engineering Japan.* 28: 186-192.

[18] Schaep, J., C. Vandecasteele, A. W. Mohammad, and W. R. Bowen. 2001. Modelling the Retention of Ionic Components for Different Nanofiltration Membranes. *Separation and Purification Technology.* 22-23: 169-179.

[19] Krantz, W. B., and G. Y. Chai. 1994. Formation and Characterization of Polyamide Membranes via Interfacial Polymerization. *Journal of Membrane Science.* 93: 175-192.